$CuInS_2$ Films for Photovoltaic Applications Deposited by a Low-Cost Method

T. Todorov,*,† E. Cordoncillo,† J. F. Sánchez-Royo,‡ J. Carda,† and P. Escribano†

Departamento de Química Inorgánica y Orgánica, Universidad Jaime I, 12071 Castellón de la Plana, Spain, and Instituto de Ciencia de los Materiales, Universitat de Valencia, c/Dr. Moliner 50, 46100 Burjassot, Valencia, Spain

Received March 20, 2006

We report an atmospheric-pressure deposition method for preparing well-adhered and compact $CuInS_2$ films. The precursor film is obtained by a solution-coating technique and is subjected to a low-cost and safe one-step reduction−sulfurization treatment. A maximum thickness of 300 nm is achieved per layer, and up to three layers were sulfurized at a time. The obtained films were characterized by X-ray diffraction (XRD), X-ray photoelectron spectroscopy (XPS), scanning electron microscopy (SEM) and visible−near-infrared (vis−NIR) spectrophotometry.

1. Introduction

If human civilization is to achieve sustainable development, it must urgently find a replacement for fossil fuels. The direct conversion of sunlight into electricity is a preferred method for clean and safe energy production in the future, and solar radiation is sufficiently abundant and widespread to satisfy society's energy needs. Furthermore, photovoltaic installations are some of the most environmentally friendly and easily maintainable alternative energy converters. The main handicap to their widespread adoption is the high production price of the currently available photovoltaic modules based on crystalline silicon or vacuum-processed thin films.[1,2] New low-cost and easily scaled production technologies need to be developed before photovoltaics can contribute significantly to global energy production.

Compound thin-film solar cell technologies are expected to lead to lower processing costs while maintaining high efficiency, making photovoltaics competitive with traditional means of energy production. In this sense, thin-film chalcopyrite solar cells are promising for future large-scale production. The high absorption coefficient and adequate band gap of these materials permits high efficiencies with relatively thin absorber layers. Highest theoretical efficiency (25%)[3] is attributed to $CuInS_2$, although the experimental record (19.2%) has been achieved with CIGS [Cu(In,Ga)-$(Se,S)_2$] absorbers.[4] Pilot plants for CIGS modules employing coevaporation[5] and rapid thermal treatment of stacked elemental layers[6] are already yielding stable production with considerable efficiency. Pilot facilities for $CuInS_2$ modules are being constructed as well.[7] Important cost reduction upon upscaling of these productions is envisioned,[8] although the necessary vacuum equipment would require large capital investments.

Although low-cost methods for chalcopyrite films deposition have been reported,[9] they yield inferior film quality and cell performance. These methods include spray pyrolysis,[10−13] electrodeposition,[14,15] and nanoparticle precursors.[16−18] Compact films have been obtained from ethylcellulose paste containing metal salts treated with elemental selenium vapor,[16] in this case forming an amorphous carbon underlayer. Relatively high efficiency (13.6%) has been obtained by printing suspensions of oxide nanoparticles followed by consecutive reduction and selenization with H_2 and H_2Se.[16] In most of these low-cost methods, problems with either layer adhesion or densification arise. Furthermore, the use of H_2 and H_2S or H_2Se requires special safety precautions.

Several reports describe the conversion of oxide precursors deposited by spray pyrolysis to chalcogenide films by direct treatment with chalcogen vapor, which can be considered safer and relatively environmentally friendly. $CuInSe_2$[12,13]

* Corresponding author: phone (+34) 964 728245; e -mail krassimi@qio.uji.es.
† Universidad Jaime I.
‡ ICMUV.

(1) Surek, T. *J. Cryst. Growth* **2005**, *275*, 292.
(2) Zweibel, K. *Solar Energy Mater. Solar Cells* **2000**, *63*, 375.
(3) Siebentritt, S. *Thin Solid Films* **2002**, *403*, 1.
(4) Ramanathan, K.; Contreras, M.; Perkins, C.; Asher, S.; Hasoon, F.; Keane, J.; Young, D.; Romero, M.; Metzger, W.; Noufi, R.; Ward, J.; Duda, A. *Prog. Photovoltaics Res. Appl.* **2003**, *11*, 225.
(5) Lammer, M.; Kniese, R.; Powalla, M. *Thin Solid Films* **2004**, *451*, 175.
(6) Palm, J.; Probst, V.; Karg, F. *Solar Energy* **2004**, *77*, 757.
(7) Klenk, R.; Scheer, D.; Lux-Steiner, M.; Luck, I.; Meyer, N.; Ruhle, U. *Thin Solid Films* **2005**, *480*, 509.
(8) Powalla, M.; Dimmler, B. *Thin Solid Films* **2000**, *361−362*, 540.
(9) Kaelin, M.; Rudmann, D.; Tiwari, A. *Solar Energy* **2004**, *77*, 749.
(10) Oja, I.; Nanu, M.; Katerski, A.; Krunks, M.; Mere, A.; Raudoja, J.; Goosens, A. *Thin Solid Films* **2005**, *480−481*, 82.
(11) Hollingsworth, J.; Banger, K.; Jin, M.; Harris, J.; Cowen, J.; Bohannan, E.; Switzer, J.; Buhro, W.; Hepp, A. *Thin Solid Films* **2003**, *431−432*, 63.
(12) Weng, S.; Cocivera, M. *J. Appl. Phys.* **1993**, *74*, 2046.
(13) Beck, M.; Cocivera, M. *Thin Solid Films* **1996**, *272*, 71.
(14) Taunier, S.; Grand, P.; Chomont, A.; Ramdani, O.; Naghavi, N.; Hubert, C.; Mahe, E.; Kerrec, O. et al. *Thin Solid Films* **2005**, *480−481*, 526.
(15) Bhattacharya, R.; Hiltner, J.; Batchelor, W.; Contreras, M.; Noufi, R.; Sites, J. *Thin Solid Films* **2000**, *361*, 396.
(16) Kaelin, M.; Rudmann, D.; Kurdesau, F.; Zogg, H.; Meyer, T.; Tiwari, A. *Thin Solid Films* **2005**, *480*, 486.
(17) Eberspacher, C.; Friedrich, C.; Pauls, K.; Serra, J. *Thin Solid Films* **2001**, *387*, 18.
(18) Kapur, V.; Bansal, A.; Asensio, I. *Thin Solid Films* **2003**, *431*, 53.

10.1021/cm0606631 CCC: $33.50
Published on Web 06/03/2006

and CdS[19] were successfully obtained from oxide films without the use of additional reducing gases.

With some exceptions,[10] most of the low-cost approaches to absorber materials have been focused on selenide-based materials and their doping with elements such as Ga in order to tune the optical band gap to the optimal for solar energy conversion (1.5 eV), which is inherent to pure $CuInS_2$.

This paper reports a low-cost and safe route for synthesizing $CuInS_2$ films by use of amorphous oxide precursor film deposited by a soft-chemistry method. The substrates are coated with triethanolamine-ethanol solutions of Cu(II) and In(III) acetates and subjected to a reduction−sulfurization treatment with ethanol-saturated nitrogen and elemental sulfur.

Previous work on soft-chemistry methods for copper-oxide film deposition reports the use of mono- and diethanolamine copper(II) acetate complexes.[20] While smaller crystal size was obtained with diethanolamine, the reasons for this were not discussed. Two possible explanations could be the better chelating ability of diethanolamine and the fact that the rate constant of the reduction of Cu(II)-amine complexes was found to increase in the order mono- < di- < triethaolamine (TEA).[21] The authors explain this with the increasing ionicity (α^2) of the Cu−amine bond from primary to secondary to ternary amine. Hence it would be even easier to reduce the Cu^{2+} ion in a tertiary amine. Other authors also report that Cu(I) may be present in TEA complexes of this metal because some of the alcohol functions on the ligands may be oxidized, possibly to aldehyde.[22] Following this rationale, we decided to use TEA as a polydentate ligand. Furthermore, its indium(III) complex has demonstrated to be effective for the synthesis of mesoporous oxide structures.[23] This chelating agent is already widely used in industry for being cheap, abundant, and environmentally tolerable.[24]

To avoid a separate treatment and to favor the reduction reactions during the atmospheric pressure sulfurization process, we introduced ethanol vapor as a reducing agent in the N_2 carrier gas.

The whole process is carried out at atmospheric pressure without the use of toxic or inflammable gases, thus reducing the health hazards as well as the materials and equipment costs. Although we have used the spin-coating technique, any standard coating method such as spraying, printing, or dipping can be used, achieving almost complete material utilization.

2. Experimental Section

2.1. Reagents. All reagents used for the deposition were analytical grade: copper(II) acetate monohydrate, $Cu(CH_3COO)_2 \cdot H_2O$, (98%, Aldrich); indium(III) acetate, $In(CH_3COO)_3$, (99.99%, Aldrich); triethanolamine [tris-(2-hydroxyethyl)amine, TEA], (99%, Riedel-de Haen); ethanol, CH_3CH_2OH, (99.8%, Scharlau); sulfur, S (99.5%, J. P. Baker).

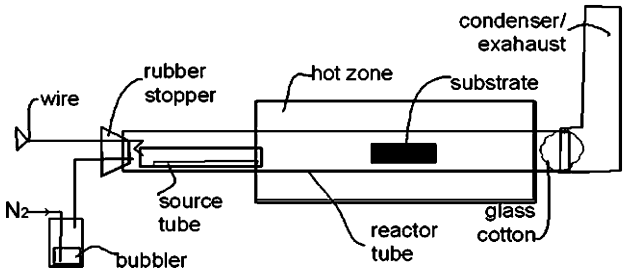

Figure 1. Experimental setup for the reduction−sulfurization process.

2.2. Preparation of the Coating Solution. Copper(II) acetate monohydrate and indium(III) acetate were dissolved into a TEA/water/ethanol solution. The Cu:In:TEA:H_2O:ethanol ratio was 1:1:5:4:26. The mixture was first stirred for 4 h at 60 °C and then for 24 h at room temperature. The obtained transparent deep-blue solution was used directly (samples A and B) or diluted with ethanol to deposit thinner layers (sample D).

2.3. Film Deposition. Glass slides (Menzel-glaser) were used as substrates. Prior to deposition, the substrates were ultrasonically cleaned in a water−detergent solution and then washed with distilled deionized water and ethanol.

The samples were spin-coated (Chemat Technology KW-4A coater) at 2000 rpm for 1 min, preceded by spin-up at 500 rpm for 2 s. The obtained transparent films were heat-treated consecutively on two separate hot plates. The first one was maintained at 250 °C to eliminate the solvents and to initiate precursor decomposition, upon which the films turned reddish-brown. The second plate was adjusted by use of an infrared thermometer (Scantemp ST80XB) so that the surface of the films was maintained at 350−360 °C. During the 5-min process, the samples turned transparent with a slightly brownish hue. The coating cycle was repeated 1−3 times for concentrated solutions (samples A1,2,3 and B1,2,3, respectively) and 8 times for the solution diluted with an equal volume of ethanol (sample D).

2.4. Sulfurization. The samples were subjected to a novel one-step reduction−sulfurization process using ethanol-saturated nitrogen gas and elemental sulfur. The reactor (Figure 1) consisted of a 50 cm-long borosilicate glass tube inserted in a tubular oven. A glass bubbler filled with ethanol was connected to the inlet pipe. The sulfur source consisted of a smaller diameter 15 cm glass tube, whose position could be adjusted inside the wider tube. The outlet of the reactor was plugged with glass cotton. The hot gases that might otherwise corrode the metal parts of the oven were guided away through an exhaust tube made of aluminum foil on which most of the residual sulfur condensed. The treatments were performed under a fume hood.

In a typical experiment, the source tube was loaded with 2 g of precipitated sulfur distributed along 10 cm and set at the beginning of the hot zone of the tubular oven. The samples were heated at a rate of 20 °C/min up to the maximum temperature−450 °C for samples A, 500 °C for samples B, and 550 °C for samples C and D−in a flow of ethanol-saturated N_2 (about 0.5 L/min). During the heating, the material at the end of the sulfur source melted, initiating slow evaporation. Five minutes after the maximum temperature was reached, the sulfur source was moved manually about 1 cm at 1-min intervals for 10 min into the hot zone. At the end of this intense sulfurization treatment, the reactor was withdrawn from the oven, letting the sulfur source cool for 1 min before removal of the samples from the hot zone.

To study the reducing effect of ethanol, a three-layered sample was subjected to identical treatment at 500 °C in a clean glass tube without a sulfur source.

(19) Weng, S.; Cocivera, M. *Solar Energy Mater. Solar Cells* **1995**, *36*, 301.
(20) Oral, A.; Mensur, E.; Aslan, M.; Basaran, E. *Mater. Chem. Phys.* **2004**, *83*, 140.
(21) Kumbhar, A.; Kishore, K. *Radiat. Phys. Chem.* **2003**, *66*, 275.
(22) Whitmire, K.; Hutchison, J.; Gardberg, A.; Edwards, C. *Inorg. Chim. Acta* **1999**, *294*, 153.
(23) Emons, T.; Li, J.; Nazar, L. *J. Am. Chem. Soc.* **2002**, *124*, 8516.
(24) Kirilov, A.; Kopylovich, M.; Kirilova, M.; Haukka, M.; Guedes da Silva, M.; Pombeiro, A. *Angew. Chem.* **2005**, *117*, 4419.

Table 1. Film Processing Conditions and Average Crystal Size, Calculated by the Scherrer Equation

sample ref	no. of layers	sulfurization temp (°C)	avg crystal size by XRD (nm)
A1	1	450	36
A2	2	450	48
A3	3	450	34
B1	1	500	39
B2	2	500	56
B3	3	500	61
C	3	550	33
D	8 (diluted)	550	61
E	3	450 (3 times)	68

The sulfurization treatment conditions of the films are summarized in Table 1. The procedure was performed only once after the deposition of all precursor layers, except for sample E, which was sulfurized a total of three times after the deposition of each layer.

2.5. Characterization of the Films. The crystal structure of the films was monitored by X-ray powder diffraction (XRD) with a Siemens D5000D diffractometer equipped with a Cu Kα radiation source and Siemens Diffract Plus software, which also determined diffraction peak positions and intensities. Data were collected by step-scanning from 20° to 60° 2θ with a step size of 0.05° 2θ and 1 s counting time per step. The instrument was calibrated by use of an external Si standard, which served also as a reference for grain-size determination.

The optical transmission of the films was measured with a Cary 500 Scan UV−vis−NIR spectrophotometer. The data were registered from 400 to 1100 nm with an uncoated glass as a reference.

Film composition was studied by X-ray photoelectron spectroscopy (XPS) depth profiling. The measurements were carried out in an ultrahigh-vacuum evaporation chamber connected to an Escalab 210 multianalysis system (base pressure 1.0×10^{-10} mbar) from Thermo VG Scientific. Photoelectrons were excited with the Mg Kα line (1253.6 eV). The sample was successively sputtered by using an Ar ion gun until the film was removed from the sputtered area, allowing us to analyze the homogeneity of the sample.

Film morphology and composition were determined by scanning electron microscopy (SEM) on a scanning electron microscope (Leica Leo 440) equipped with a spectrometer for energy-dispersive X-ray microanalysis (EDX) under the following operating parameters: acceleration voltage 20 kV, measuring time 100 s, working distance 25 mm, and counting rate 1.2 kcps. The samples for microstructure and microanalysis determination were introduced by use of an aluminum holder with graphite adhesive tape. The thickness of the films was estimated from micrographs of film cross sections.

3. Results and Discussion

3.1. X-ray Diffraction. The XRD of all films pretreated in air can be assigned to an amorphous material, although a small peak in the diffraction patterns of the reddish-brown samples obtained after the first firing at 250 °C could be attributed to elemental copper. This peak disappears as films turn transparent during the heat treatment at 350 °C.

These results suggest that the reduction of Cu(II) to Cu(I) is initiated in the precursor solution as already mentioned in the Introduction. The oxidation of the organic material during the heat treatment leads to the reduction of copper to the elemental state at 250 °C that in the next firing at 350 °C generates amorphous material. The color change to transparent with a very slight brownish hue suggests that the Cu(0) is oxidized to Cu(I).[25] Hence it can be concluded that prior to sulfurization the films are composed mainly of Cu(I) and In(III) amorphous oxides, although the presence of a small amount of Cu(II) cannot be excluded.[12]

The reducing effect of ethanol vapor during the next sulfurization step is demonstrated by repeating the treatment process at 500 °C, but in a flow of ethanol-saturated N_2 with no sulfur addition. The XRD results indicate the presence of metallic copper and In_2O_3.

Thus it can be inferred that the proposed synthesis route can lead to the formation of Cu(I) through the reduction of Cu(II) complexes in solution, during the oxidation of the organic material and/or ethanol.

Figure 2 presents the diffractograms of thin-film samples after sulfurization under different conditions. The diffraction data can be summarized as follows:

The diffraction peaks can be assigned to the $CuInS_2$ crystalline structure, space group I-42d, with a preferred (112)-plane orientation, according to the JCPDS 27-159 file. In the spectra of 1A and 1B-layered films, (Figure 2, panels a and b, respectively), only (112) and (204)/(220) diffraction peaks are visible. For the rest of the samples, peaks at (004)/(200) and (116)/(312) are also observed.

Peak intensities increase with film thickness and with temperature increases from 450 to 500 °C. Contrary to our expectations, higher treatment temperatures have a much smaller effect on the intensities of the diffraction peaks than what would be expected from their improved crystallinity. This might indicate that at sulfurization temperatures as low as 450 °C the crystal quality is comparable to that of the films treated at 550 °C. On the other hand, a higher temperature reduces the full width at half-maximum (fwhm) of the (112) peak, indicating a grain-size increase.

The particle size (D) was determined with Scherrer's equation[30] for the (112) peak. The calculated average particle sizes ranged from 36 to 68 nm (Table 1).

From Table 1, it could be inferred that, apart from sample A3, the average crystal size of the thin-film samples grows with the number of layers and is also influenced by the sulfurization temperature (comparing samples A and B). The observed exception may be due to the very small fluctuations of the sulfur partial pressure in the beginning of the treatment and the multiple phase transformations occurring during this period.[26] The eight-layered sample D, prepared from a diluted solution and sulfurized at 550 °C, had a larger size (61 nm) than a typical three-layered sample C treated at the same conditions (33 nm), demonstrating the effect of the deposition procedure, probably causing difference in the diffusion rate of the sulfur. Maximum particle size (68 nm) was obtained when each layer was sulfurized individually (sample E).

Further investigation is in progress in order to optimize the sulfurization treatment and achieve larger grain size, which is preferable for photovoltaic applications.

3.2. X-ray Photoelectron Spectroscopy. XPS spectra of a three-layered film sulfurized at 500 °C was taken at

(25) Ogwu, A. *CERAC Coating Mater. News* **2003**, *13*, 4.
(26) Klopmann, C.; Djordjevic, J.; Rudigier, E.; Scheer, R. *J. Cryst. Growth* **2006**, *289*, 113.

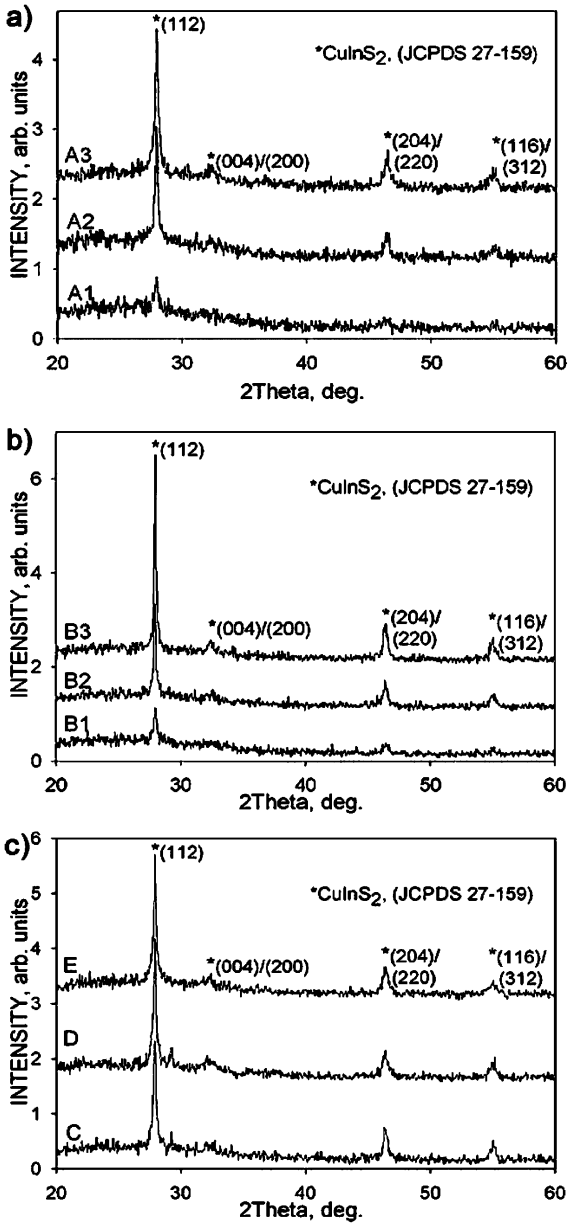

Figure 2. XRD of films prepared under different conditions: (a) A1, A2, and A3, of one, two, and three layers, respectively, sulfurized at 450 °C; (b) B1, B2, and B3, of one, two, and three layers, respectively, sulfurized at 500 °C; (c) C (three-layered) and D (eight-layered) −at 550 °C; (E) individual layers sulfurized −at 450 °C after each coating cycle.

different sputtering depths up to about 600 nm (Figure 3). The results should be considered within the known limitations associated with depth profiling techniques using ion beam sputtering.[27] Considering the difficulty of an accurate quantitative analysis,[28,29] the data represent only the distribution behavior of the elements in the bulk of the film.

As can be seen in Figure 3, after removal of the surface layers, including the area shaded by the larger grains (sputtering 2), a homogeneous distribution of the elements in the film is observed, which is almost stoichiometric

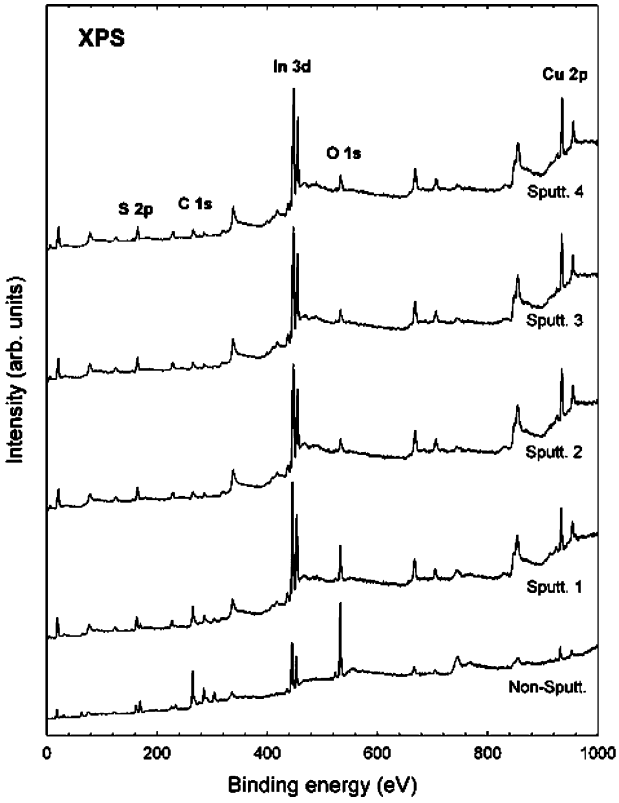

Figure 3. XPS spectra of a three-layered film sulfurized at 500 °C up to a depth of approximately 600 nm, taken before sputtering and after each of the four sputtering steps.

according to the EDX results. Copper loss from the film surface was confirmed also by EDX analysis of this specific sample and may be due to volatilization of copper sulfides during the various phase transformations accompanying sulfurization treatment, as we already commented. Low carbon and oxygen impurities on the sample surface were detected, which could not be avoided during the characterization.[29] The fact that these elements are almost absent after the second sputtering step indicates that they are not inherent to the sample.

3.3. Scanning Electron Microscopy. The surface of the amorphous oxide films before sulfurization was so smooth that no defects or defined crystallites could be observed by SEM. From cross-section images, whose resolution was very poor because of the limits of the technique, it was estimated that the crystallite size of the oxide precursor is about 10−12 nm.

Surface morphology and cross-sections of the sulfurized films are shown in Figure 4. It can be observed that the films are dense and adhered to the substrate. Except for sample E (not shown), in which the sulfurization process was applied after each coating cycle, no delamination upon fracturing can be detected by SEM. This, considering also the surface free of cracks and pinholes, is an indication of sufficient adherence to the substrate.[12]

All films had a dense bottom layer and an irregular surface of embedded grains ranging from 100 to 800 nm, depending on the deposition procedure and not on the sulfurization process. As can be seen, the size of these grains is about an order of magnitude bigger than the average crystallite size obtained by XRD. There are two possible reasons for this:

(27) Dhlamini, F.; Alberts, V. *J. Phys. Chem. Solids* **2005**, *66*, 1880.
(28) Zouaghi, M.; Nasrallah, T.; Marsillac, S.; Bernede, J.; Belgacem, S. *Thin Solid Films* **2001**, *382*, 39.
(29) Qui, J.; Jin, Z, Qian, J.; Shi, Y.; Wu, W. *J. Cryst. Growth* **2005**, *282*, 421.
(30) West, A. *Solid State Chemistry and its Applications*; John Wiley & Sons: New York, 1992.

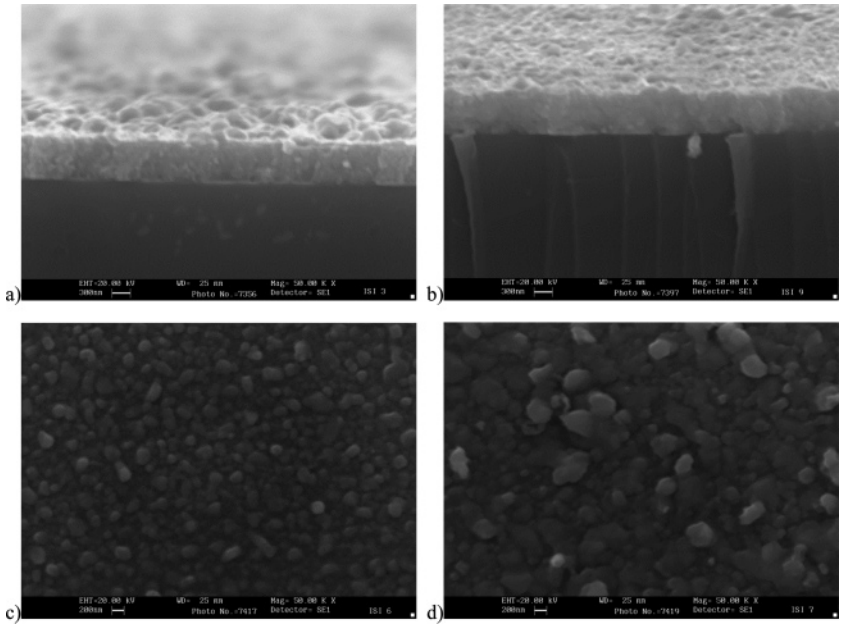

Figure 4. Micrographs of the cross-sections of samples A3 (a) and D (b) and morphology of film B1 (c) and B2 (d) surfaces.

the grains are agglomerates of smaller particles, or formation of larger crystals at the surface is caused by preferential consumption of sulfur vapor in the beginning of the process before it is able to diffuse in depth. When concentrated solution was employed, the grains were larger in the samples with more layers (Figure 4c,d). Sample D, prepared from a diluted solution (eight layers) exhibited a smoother surface (Figure 4b). Upon rupture, the bottom layer revealed particles or agglomerates of irregular shape and size with a prevailingly vertical orientation, which might indicate partial columnar growth.

The thickness of the dense layer of each sample was determined from the micrographs of the cross-sections. Thickness of up to 300, 600, or 900 nm was achieved with a single sulfurization treatment of one-, two-, or three-layered films, respectively.

The film surface composition was determined by energy-dispersive X-ray analysis (EDX). A ratio close to 1:1 of Cu to In was obtained in films prepared at 500 °C, although high reproducibility of this ratio was obtained only in bulk (determined by EDX spot analysis of film cross section) while the surface composition in repeated experiments could show slight Cu deficiency. Apart from the eight-layered sample D, all films, whether prepared at lower or higher temperatures, had indium-rich surfaces. We attribute this copper loss to volatilization of some species during the several phase transformations that occur during the sulfuization treatment.[26] The obtained results were further related to the optical band gap of the samples (Figure 7).

As already mentioned, further investigation is in progress in order to optimize sulfurization treatment and achieve both larger grain size and better control of surface composition.

3.4. Optical Properties. Figure 5 displays the room-temperature transmission spectra for all obtained thin films. The data were recorded in the wavelength range of 400−1100 nm.

From these graphs it can be concluded that, even in one-layered films (A1 and B1), a significant part of the visible spectrum is absorbed (Figure 5a). Film C, having three layers, shows a higher absorption than film D, which is of similar thickness but was obtained from a diluted solution and eight coating cycles. The optical transmission of typical three-layered films was less than 5% in the visible spectrum, which could be considered acceptable for photovoltaic applications.

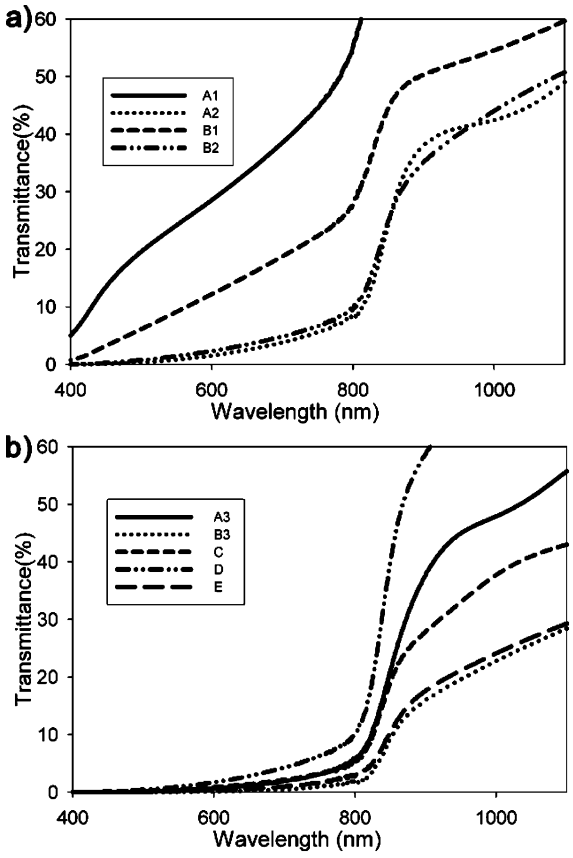

Figure 5. Optical transmittance spectra of (a) one and two-layered films; (b) three-layered films.

The optical band gaps of the films were determined by use of the transmission data together with film thickness determined by SEM. According to an established method,[19]

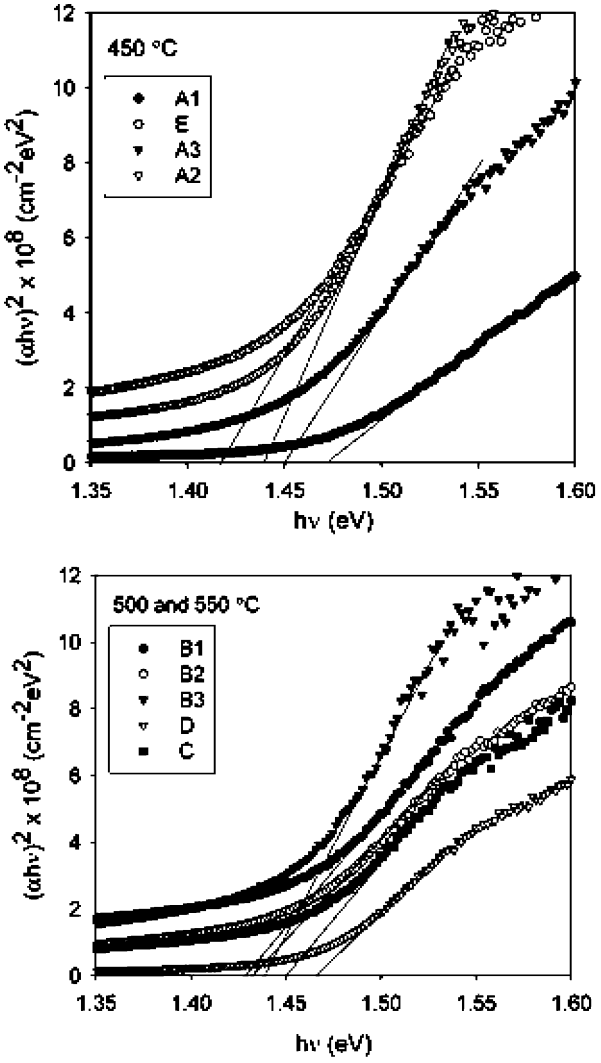

Figure 6. Plot of $(\alpha E)^2$ vs E: (a, top panel) samples sulfurized at 450 °C; (b, bottom panel) samples sulfurized at 500 and 550 °C.

$(\alpha E)^2$ was plotted against E, where α is the absorption coefficient and E is the corresponding photon energy $h\nu$, as seen in Figure 6.

The obtained values range from 1.42 to 1.47 eV, being slightly lower than those of monocrystalline $CuInS_2$ (~1.53 eV) but adequate for photovoltaic applications and comparable to those obtained by other deposition methods.[11,31] Although a study of intentionally varied Cu/In ratio on the properties of the films will be published elsewhere, the limited copper loss during the sulfurization treatment observed in this work influences the optical band gap value. This fact could be observed in Figure 7, in which the Cu/In ratio decrease leads to a band gap increase. This trend has already been reported by other authors.[32] It can be summarized that the band gap values increase when the particle size and the Cu/In ratio decrease. As observed in other semiconductor systems, the optical absorption blue shift is associated with quantum confinement effects.[33,34]

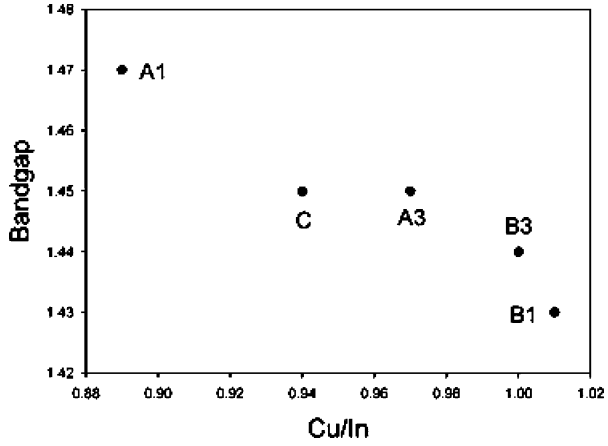

Figure 7. Relationship between film surface composition and optical band gap.

After the treatment optimization is completed, the next step of our work will study the properties of these films in complete solar cells.

4. Conclusions

Single-phase compact $CuInS_2$ films have been deposited successfully at atmospheric pressure by coating a precursor layer from solution and subjecting it to a novel reduction−sulfurization technique. Although further treatment and precursor composition optimization is required in order to increase grain size, films with high optical absorption and a band gap adequate for photovoltaic applications were prepared with simple and inexpensive equipment. No toxic or inflammable gases were used. The method is suitable for industrial production, permitting fast, cheap, and safe deposition of large-area absorbers for photovoltaic modules.

Acknowledgment. This work has been supported by the Spanish Ministry of Education and Science through predoctoral scholarship FPU AP-2004-6965, by Bancaja Foundation-UJI through Project P1-1B2003-27, and by Generalitat Valenciana through Group Project 05/006.

CM0606631

(31) Krunks, M.; Bijakina, O.; Varema, T.; Mellikov, E. *Thin Solid Films* **1999**, *338*, 125.

(32) Hou, X.; Choy, K. *Thin Solid Films* **2005**, *480*, 13.

(33) Brus, L. J. *Chem. Phys.* **1984**, *80*, 4403.

(34) Cordoncillo, E.; Escribano, P.; Monrós, G.; Tena, M. A.; Orera, V.; Carda, J. *J. Solid State Chem.* **1995**, *118*, 1.